

Magnitude, Impact, and Management of Respiration-induced Target Motion in Radiotherapy Treatment: A Comprehensive Review

S. A. Yoganathan, K. J. Maria Das, Arpita Agarwal, Shaleen Kumar

Department of Radiotherapy, Sanjay Gandhi Postgraduate Institute of Medical Sciences, Lucknow, Uttar Pradesh, India

Abstract

Tumors in thoracic and upper abdomen regions such as lungs, liver, pancreas, esophagus, and breast move due to respiration. Respiration-induced motion introduces uncertainties in radiotherapy treatments of these sites and is regarded as a significant bottleneck in achieving highly conformal dose distributions. Recent developments in radiation therapy have resulted in (i) motion-encompassing, (ii) respiratory gating, and (iii) tracking methods for adapting the radiation beam aperture to account for the respiration-induced target motion. The purpose of this review is to discuss the magnitude, impact, and management of respiration-induced tumor motion.

Keywords: Dynamic multileaf collimator, four-dimensional computed tomography, gating, internal target volume, lung, respiratory motion, tracking

Received on: 14-02-2017

Review completed on: 31-05-2017

Accepted on: 11-07-2017

INTRODUCTION

Radiotherapy is most commonly used treatment method for effective management of many cancers including lung cancer, and it remains the most cost-effective way of curing many cancers. The goal of radiotherapy is to apply radiation to eradicate tumor while sparing normal tissues, and this is not always easy to achieve due to various types of uncertainties associated with the external beam radiotherapy treatment process. Among various sources of uncertainties, intrafractional respiratory motion is the primary focus of this review.

Respiration is an involuntary physiological process by which the oxygen is delivered to the cells from the external environment and the carbon dioxide is transported in the opposite direction. Due to respiration, the organs in thoracic and upper abdomen regions such as lungs, liver, pancreas, esophagus, and breast move. In addition, prostate and kidneys are also known to move due to respiration. Respiration-induced motion is a significant factor for geometric and dosimetric uncertainties during imaging, treatment planning, and treatment delivery of thoracic and abdominal radiotherapy.^[1]

Although 5-year survival rate of many cancers has improved considerably in line with the technology development, the same for lung and bronchus cancer remains 18.1%.^[2] Interestingly, there is clinical evidence for local control and survival improvement at higher radiation dose levels^[3,4] and altered dose fractionation schemes.^[5,6] However, to compensate the respiration-induced target motion, traditionally, treatment field aperture is opened wide enough to encompass entire target motion trajectory;^[7] this leads to increased field margin. Inclusion of excess normal tissues increases the normal tissue complications, and this is one of the main hindrances for dose escalation.

Respiratory motion complicates treatment, and thus, concept of “time” has been introduced as the fourth dimension in radiotherapy. Recent developments in radiation therapy have

Address for correspondence: Dr. S. A. Yoganathan,
Department of Radiotherapy, Sanjay Gandhi Postgraduate Institute of
Medical Sciences, Rae Bareilly Road, Lucknow - 226 014,
Uttar Pradesh, India.
E-mail: sayoganathan@yahoo.co.in

This is an open access article distributed under the terms of the Creative Commons Attribution-NonCommercial-ShareAlike 3.0 License, which allows others to remix, tweak, and build upon the work non-commercially, as long as the author is credited and the new creations are licensed under the identical terms.

For reprints contact: reprints@medknow.com

How to cite this article: Yoganathan SA, Maria Das KJ, Agarwal A, Kumar S. Magnitude, impact, and management of respiration-induced target motion in radiotherapy treatment: A comprehensive review. *J Med Phys* 2017;42:101-15.

Access this article online

Quick Response Code:



Website:
www.jmp.org.in

DOI:
10.4103/jmp.JMP_22_17

resulted in following technical solutions for adapting the radiation beam aperture to account for the respiration-induced target motion:

1. Motion-encompassing method
2. Respiratory gating
3. Tracking.

The purpose of this review article is to summarize the magnitude of respiration-induced tumor motion, its effect and management. This article is organized into three parts. Magnitude and impact of respiration-induced tumor motion are discussed in first two sections. The third part is devoted to discussing different means of respiratory motion management techniques.

MAGNITUDE OF RESPIRATION-INDUCED TARGET MOTION

The extent of respiration-induced target motion is mainly measured using the tools such as fluoroscopy,^[8-11] computed tomography (CT),^[12] and magnetic resonance imaging (MRI).^[13]

Table 1 shows the summary of respiration-induced lung tumor motion. In general, the lung tumor displacement is not isotropic and is predominantly in the craniocaudal direction.^[8,13] Mageras *et al.*^[14] evaluated the lung tumor motion characteristics using four-dimensional CT (4DCT). They found that the tumor motion was more than 1 cm for seven cases out of 12, primarily in the craniocaudal direction. Lung tumor motion is related to target volume and location. Yu *et al.*^[12] compared lung tumor motion characteristics in non-small cell lung cancer patients between early and locally advanced stage using 4DCT and also determined the tumor motion relation with position, volume, and diaphragm motion. They observed that the tumor motion (95th percentile) was greater by more than 50% in early-stage group than locally advanced lung cancer group. Early tumors situated in lower lobe showed the maximum displacement (median: 9.2 mm)

compared to upper and middle lobe tumors which showed less motion (median: 3.3 mm).

In addition to lung, abdominal tumors such as in the esophagus,^[15,16] liver,^[17,18] pancreas,^[19-21] and kidneys^[22-24] also tend to move due to respiration [Table 2]. Similar to lung tumor motion, respiration-induced abdominal tumor motion is also primarily in the craniocaudal direction. Motion characteristics of kidneys revealed a complex pattern and were observed to be strongly related to respiration.^[22-24] The right kidney tends to move more than the left kidney due to the proximity of the liver.^[23] Detailed summary of kidney motion can be found in the recent review by Pham *et al.*^[24] Prostate is also known to move with respiration,^[25,26] and this could be significantly reduced in supine patients when the thermoplastic shells were removed.

IMPACT OF RESPIRATION-INDUCED TARGET MOTION DURING RADIATION TREATMENT DELIVERY

Intra- (during the fraction) and inter-fractional (between fractions) motion of tumor/target causes geometric and dosimetric uncertainties in the radiation therapy treatment delivery.^[28] The intrafractional motion is mainly due to respiration. Respiration-induced target motion would produce a dose blurring at field edge in a static radiotherapy beam, whereas in dynamic treatments, the effect would be entirely different.

For example, in a dynamic intensity-modulated radiotherapy (IMRT) delivery, along with the collimator (multileaf collimator [MLC] or jaw), the tumor is also moving in sites such as lung and upper abdomen which introduces the interplay effect; due to this, the delivery becomes more challenging. These uncertainties negate the real benefit offered by IMRT unless compensated.

Dosimetric effect of respiration-induced target motion in radiation therapy was reported earlier. One of the first studies

Table 1: Respiration-induced lung tumor motion

Author	Technique	Description	AP	ML	CC
Shimizu <i>et al.</i> ^[9] (4 patients)	Real-time tumor-tracking system (fluoroscopy)	Range	8.1-14.6	5.5-10.0	6.8-15.9
Chen <i>et al.</i> ^[10] (20 patients)	Fluoroscopy	Range	-	-	0.0-50.0
Seppenwoolde <i>et al.</i> ^[8] (20 patients)	Real-time tumor-tracking system (fluoroscopy)	Mean (range)	2.5 (0.0-8.0)	1.5 (0.0-3.0)	5.8 (0.0-25.0)
Sixel <i>et al.</i> ^[11] (10 patients)	Digital fluoroscopy integrated with CT simulation	Range	0.0-5.0	0.0-4.0	0.0-13.0
Erridge <i>et al.</i> ^[27] (25 patients)	Orthogonal portal images acquired at random points in the breathing cycle	Mean (range)	9.4 (4.8-21.5)	7.3 (3.2-12.3)	12.5 (4.7-33.8)
Yu <i>et al.</i> ^[12] 191 (94 early stage, 97 locally advanced)	4DCT	Early-stage 95 th percentile (median)	6.8 (2.9)	3.9 (1.0)	18.3 (4.2)
		Advanced stage 95 th percentile (median)	5.1 (2.0)	3.9 (1.0)	11.7 (3.3)
Plathow <i>et al.</i> ^[13] (20 patients)	Dynamic MRI	Lower lobe mean (range)	6.1 (2.5-9.8)	6.0 (2.9-9.8)	9.5 (4.5-16.4)
		Middle lobe mean (range)	4.3 (1.9-7.5)	4.3 (1.5-7.1)	7.2 (4.3-10.2)
		Upper lobe mean (range)	2.8 (1.2-5.1)	3.4 (1.3-5.3)	4.3 (2.6-7.1)

All data are shown in mm. AP: Anterior-posterior, ML: Mediolateral, CC: Craniocaudal, MRI: Magnetic resonance imaging, CT: Computed tomography
4DCT: Four-dimensional CT

Table 2: Respiration-induced target motion (mean) in abdomen and pelvis

Author	Technique	Site	AP	ML	CC
Lever <i>et al.</i> ^[15] (36 patients)	Cine MRI	Esophagus	4.9±2.5	2.7±1.2	13.3±5.2
Patel <i>et al.</i> ^[16] (30 patients)	4DCT	Esophagus	2.8±2.0	2.2±2.3	8.0±4.5
Brix <i>et al.</i> ^[17] 5 healthy volunteers	Real-time MRI	Liver	2.5	1.6	11.0
Park <i>et al.</i> ^[18] (20 patients)	4DCT	Liver	5.1±3.1	3.0±2.0	17.9±5.1
	CBCT (with fiducials)		5.3±3.1	2.8±1.6	16.5±5.7
Feng <i>et al.</i> ^[19] (17 patients)	Cine MRI	Pancreas	8.0±3.0 (anterior)	-	20.0±10.0
			6.0±2.0 (posterior)		
Goldstein <i>et al.</i> ^[20] (30 patients)	4DCT	Pancreas	3±1.7	3±1.8	5.5±2.3
Knybel <i>et al.</i> ^[21] (20 patients)	Synchrony® respiratory tracking system	Pancreas	3.8 (2.9-8.2)	3.4 (2.6-6.7)	11.1 (4.8-23.4)
Yamashita <i>et al.</i> ^[22] (20 patients)	Spiral 4DCT	Kidney	3.6±2.1	1.7±1.4	11.1±4.8
Abhilash <i>et al.</i> ^[23] (48 healthy patients and 62 affected patients)	Ultrasound	Right kidney	-	13.6±3.7	24.54±6.4
		Left kidney	-	9.8±3.3	17.1±3.7
Malone <i>et al.</i> ^[25] (40 patients in prone position)	Fluoroscopy	Prostate	1.6±1.1	-	2.9±1.7

All data are shown in mm. AP: Anterior-posterior, ML: Mediolateral, CC: Craniocaudal, MRI: Magnetic resonance imaging, 4DCT: Four-dimensional computed tomography, CBCT: Cone-beam computed tomography

was carried out by Yu *et al.*^[29] who simulated the interplay effect (parallel direction to MLC leaf motion) on a single-field IMRT based on MLC. The simulations were done for different velocities of target motion and MLC motion as well as different field width. The dose variation was considerable, and this strongly depends on the speed of the MLC motion relative to the target motion. They also found that the dose deviation increased with the decrease of beam width. In addition, they also investigated the influence of fractionation on the interplay effect and found that the dose error was reduced to 10% when considering thirty fractions. Similarly, Pehler *et al.*^[30] demonstrated that the magnitude of interplay effect in a single dynamic wedge treatment would be 15%.

In a noteworthy work, Bortfeld *et al.*^[31] conducted a statistical evaluation on the effect of intrafractional motion on IMRT dose delivery, and showed that the effect of respiratory motion on an IMRT delivery is negligible (<1%) when we consider entire course of treatment, i.e., thirty fractions, and this effect is independent of delivery techniques. Similarly, in an experimental investigation, Jiang *et al.*^[32] showed that the maximum dose deviation was up to 30% and 18% for single field and fraction; this was reduced to <1%–2% after thirty fractions.

Although the dosimetric errors of respiratory motion averaged out over thirty fractions, it is intuitive to ponder that it may be a concern in the advanced treatment regime (stereotactic body radiotherapy [SBRT]) which utilizes fewer fractions. However, it was recently shown that the respiratory motion effect on SBRT treatment delivery is also negligible.^[33-36] Li *et al.*^[33] evaluated the dosimetric effect of interplay between the tumor respiratory motion and dynamic multileaf collimator (DMLC) motion in a volumetric modulated arc therapy (VMAT) delivery of lung SBRT treatment (60 Gy in 3 fractions) by a flattening filter-free (FFF) linac (TrueBeam, Varian Medical Systems). They included six lung cancer patients who had motion range 0.5–1.6 cm, and the planning study was carried

out on 4DCT scans using two-arc VMAT plans. The control points of original static VMAT plans corresponding to each respiratory cycle were calculated, and ten new VMAT plans were generated. Deformable image registration was used to accumulate the four-dimensional (4D) dose distribution of ten VMAT plans. Although the target (Gross Tumor Volume [GTV] + 5 mm) coverage decreased with increased respiratory motion amplitude, the overall dose deviation (<3.2%) was insignificant. They concluded that the dosimetric impact of interplay effect on target coverage was insignificant in lung SBRT with FFF-based VMAT delivery.

Mutaf *et al.*^[37] simulated the dosimetric effect of irregular motion of lung tumors in 23 patients. Evaluations were carried out with two types of respiration irregularities; characteristic (random fluctuations in determination of the target motion) and uncharacteristic motions (systematic errors in determination of the target motion). Characteristic motions resulted in minimal deviation in target coverage (2.5% ± 0.9%) for the targets moving at 2 cm amplitude, and these types of motions showed 50% variation in the amplitude within a session. However, the uncharacteristic irregular motion showed larger variation in the target dose (9.6% ± 1.7%) for 2 cm amplitude. They concluded that among all types of irregular respiration, the uncharacteristic irregular motion was a clinically significant source of dosimetric uncertainty. In addition to lung, breast^[38] and prostate^[39] motion would also create dosimetric uncertainties.

Most of the studies concluded that the respiratory motion-induced dosimetric uncertainties were larger for single field or fractions and averaged out over the entire treatment delivered over several fractions. However, this effect may be different for different patient respiratory parameters such as breathing amplitude, phase, and period. This was shown by Berbeco *et al.*^[40] who measured the interplay effect in lung IMRT treatment using radiographic (Extended Dose Range 2 [EDR2]) films. Films were placed over a phantom which was programmed to simulate

a sinusoidal motion (2 cm peak-to-peak amplitude and 4 s breathing period) in the craniocaudal direction (perpendicular to leaf motion), and five field lung IMRT plans were delivered on the moving phantom. Static delivery was compared with the measurement with target motion. It was observed that the standard deviation of the dose due to interplay was <2%–4% for high-dose region on a day-to-day basis. However, when thirty fractions were considered, these were reduced to <1%. On the other hand, the minimum dose of moving target was reduced to 6% compared to static even after thirty fractions. Similarly, Mohn and Wasbø^[41] also pointed out that the dose deviation reduction (averaging) with increasing number of fractions is plan and patient specific, and this should be evaluated before the final clinical decision.

Advanced techniques such as gating and tracking can be employed to manage the respiration-induced target motion. The use of these techniques is encouraged only if considerable benefits are expected over the entire treatment course. Experimental measurement of dosimetric uncertainties of respiratory motion is laborious, and to have an idea about these dosimetric uncertainties, a patient-specific computational model is also reported.^[42]

SOLUTIONS FOR THE MANAGEMENT OF RESPIRATION-INDUCED TARGET MOTION IN RADIOTHERAPY

Recent developments in radiotherapy have resulted in various technical solutions for dealing with the respiratory motion, i.e., motion-encompassing, breath-hold, gating, and tracking method.

Motion-encompassing method

Intrafractional organ motion is an important issue in the era of conformal radiation therapy. The respiratory motion varies with respect to site, size, and shape of the organs and tissues during each session of treatment. If it is not accounted for, the tumor may be underdosed as well as normal tissue sparing may be also compromised; therefore, a safety margin called internal margin (IM) is added to CTV.^[7] CTV plus IM forms the internal target volume (ITV), and Figure 1 shows the ITV defined by ICRU 62. Optimal ITV must be used for better therapeutic ratio. Various techniques such as fluoroscopy, CT (slow, breath-hold, and 4DCT), and cone beam computed tomography (CBCT) were explored for defining the ITV.^[43]

Sixel *et al.*^[11] used a digital fluoroscopy integrated with CT scanner to measure the motion of lung tumor for deriving ITV. The fluoroscopic data were overlaid with digitally reconstructed radiographs to assess the tumor motion, and this approach is helpful in designing optimal patient-specific margin. The fluoroscopy-based tumor motion evaluation has many disadvantages (limited to two-dimensional [2D] motion, it is applicable to tumors which are visible in fluoroscopy). Therefore, CT-based tumor motion assessment techniques were evolved.

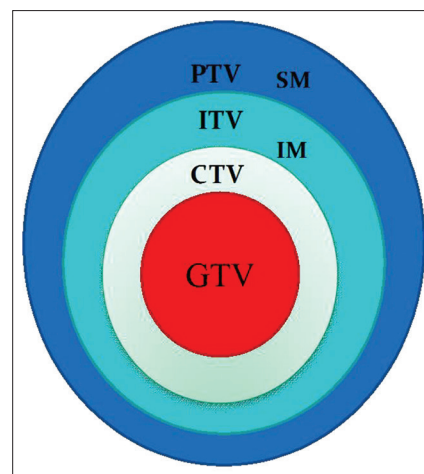


Figure 1: The internal target volume defined by ICRU 62

Lagerwaard *et al.*^[44] used multiple slow CT scans for determining ITV. The ITV volumes obtained with slow scan were always larger, and it was observed to be more reproducible. This indicated the potential use of slow scans in capturing the tumor movement. Wurstbauer *et al.*^[45] evaluated possibility of using slow CT for delineating tighter margins in external beam treatment planning of lung cancer. They showed that the slow CT scan resulted in larger ITV compared to fast CT scan. Shih *et al.*^[46] conducted a study to determine the expansion margins (IMs) beyond individual GTVs which were defined by (1) fast scan at shallow-free breathing, (2) breath-hold scans at the end of tidal volume inspiration and expiration, and (3) 4-s slow scan. The GTV was contoured on each CT scan, and the composite GTV was generated by combining all. Margins necessary to encompass the composite GTV beyond individual GTVs defined by either fast scan at quiet free breathing, breath-hold scans, or the 4-s slow scan at quiet free breathing were defined as expansion or IMs. It was observed that the expansion margins required to approximate the composite GTV in 95% of cases were 13, 10, and 5 mm for the GTVs of a single fast scan, 4-s slow scan, and breath-hold scans, respectively. They concluded that the GTV defined with breath-hold scans at the end of tidal volume inspiration and expiration has a narrower range of IMs in all directions than that of either a single fast scan or 4-s slow scan.

The slow CT scan may be better than fast CT scan for ITV definition; however, it has certain limitations. The main disadvantage of slow CT scan is the loss of resolution and contrast due to motion blurring, which leads to larger inter-observer errors in tumor and critical organ delineation. Technical advancements resulted in 4DCT for defining the tumor mobility accurately. 4DCT technique images multiple respiratory states within one data acquisition. The basic principle involves temporally oversampling data acquisition at each couch/slice position [Figure 2]. The 4DCT scan captures the changes in target position and shape, which are quantified as a function of the respiratory cycle. The respective respiratory phase at the time of image acquisition is digitally “stamped” on each CT image.

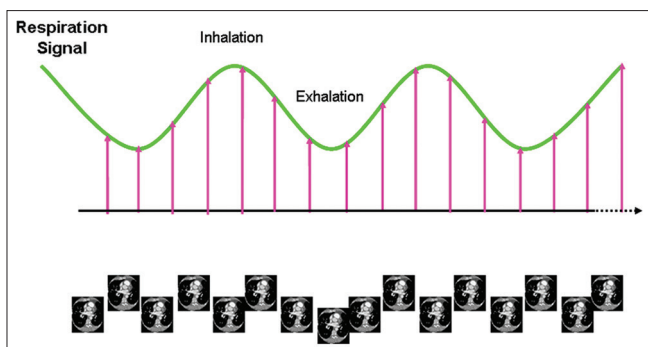


Figure 2: Principle of four-dimensional computed tomography image acquisition

Once the 4DCT scan is performed, 4D software automatically sorts the images into individual three-dimensional (3D) image sets, each representing the entire patient's anatomy during a single respiratory phase. This enables tumor and organ movement to be visualized and utilized for determination of individualized margins for treatment planning.

Underberg *et al.*^[47] compared multiple standard CT scan (six numbers) generated ITV with a 4DCT-generated ITV in ten patients. They observed that ITV resulted by 4DCT was not significantly different from multiple CT scan ITVs in eight patients, whereas for two patients who had larger target motions, the 4DCT ITV was noticeably larger. Further, combined ITVs were also generated by adding the multiple CT scan ITVs with 4DCT ITVs. Twenty-two percent of multiple CT scan ITVs were not overlapping with combined ITVs whereas this was 8.3% for 4DCT. They concluded that a 10 mm margin with a single CT scan is inadequate, and the six fast scan ITVs were comparable or smaller than a single 4DCT scan ITV. In another study, Underberg *et al.*^[48] used maximum intensity projection (MIP) technique for determining ITV from multiple phases of 4DCT. This reduces the workload of contouring the tumor and critical organs in multiple data set (often ten phases). They observed that the ratio of ITVs generated from all ten phases to those from MIP scans was 1.04 and the corresponding center of mass of both ITVs differed by <1 mm. They concluded that MIP can be a reliable tool in generating ITV. Wang *et al.*^[49] compared the 4DCT, fast helical CT, and multiphase CT (fast CT, end-inspiration and end-expiration breath-hold CT) for ITV definition and daily target coverage in SBRT. They observed that the 4DCT consistently resulted in lesser ITV than other scans and concluded that SBRT treatment planning based on 4DCT decreased the normal lung dose with adequate target coverage when it is used in conjunction with image guidance.

Studies were also attempted to use treatment verification imaging such as CBCT for defining ITV. Wang *et al.*^[50] demonstrated the feasibility of verifying the ITV of 4DCT with onboard free-breathing CBCT. They demonstrated this technique in phantom experiments and also in patient cases. The planning ITV was determined using ten phases of 4DCT scans, and the localization accuracy of CBCT was assessed by comparing the CBCT ITV with 4DCT ITV. They

observed that the localization accuracy between ITVs of 4DCT and CBCT was <1 mm and ITV deviation was <8.7% for phantom experiments. For patient cases, the deviation was within 8.0%. This study demonstrated that CBCT can be used to localize ITV for moving targets (because CBCT acquisition is similar to slow CT [gantry rotation is slow]). In a recent study, Wang *et al.*^[51] also compared 3D CBCT with 4DCT MIP (segmentation based on gradient method) for ITV localization and found that the 4DCT MIP was generally larger than (10%) those obtained with CBCT. They also observed that maximum difference in centroid position was <1.4 mm between two modalities.

In addition to radiological imaging, nuclear medicine functional imaging was also used for ITV definition. Chang *et al.*^[52] used a static positron emission tomography (PET)/CT scan to determine the ITV. The PET image was described as a consequence of a joint convolution of an ideal PET image (free from motion and partial volume effect) with a motion-blurring kernel (MBK) and partial volume effect. Using the deconvolution process, the MBK and an ITV were estimated. The feasibility of this method was evaluated on phantom experiments as well as patient studies. The ITV of PET/CT was compared with the ITVs of 4DCT and better concordance was observed. They concluded that their approach, i.e., a single static PET/CT scan has the potential to replace the 4DCT for determining ITV. Callahan *et al.*^[53] evaluated the 4DPET imaging for deriving the ITV of moving tumors and concluded that the free-breathing PET/CT always underestimates the ITV in comparison to 4D PET/CT. Further, they also validated the 4D PET MIP approach for ITV volume contouring and found that it was closely matching with the MIP resulted from 4DCT.

Lung radiotherapy treatment is usually planned with a single 4DCT acquisition and this may or may not be accurate. Guckenberger *et al.*^[54] evaluated the adequacy of a single 4DCT to characterize the lung tumor motion in SBRT treatments. In their study, four repeated 4DCT acquisitions were acquired for ten patients with 10 min interval, and the target motion variation in each scan was analyzed. They concluded that a single 4DCT scan was sufficient for majority of cases; however, larger discrepancies were observed for the lower lobe tumors and pulmonary compromised cases. Dosimetric effect of interfractional variation of lung tumor motion and volume was also analyzed using repetitive 4DCT. Britton *et al.*^[55] evaluated the geometric and dosimetric effect of interfractional variation of respiratory motion and volume in non-small cell lung cancer treatments. Although the observed dosimetric changes (ITV dose <3%) were small, they recommended the use of image-guided treatment and repeated imaging to know the interfractional changes in tumor motion and volume during treatment course.

It is important to verify the accuracy of IM during/before treatment delivery. Guckenberger *et al.*^[56] described a novel method that can be used to verify the IM of liver tumors. In their

method, the liver volumes were contoured on end-inhalation and end-exhalation CT scans derived from a 4DCT and on the CBCT scans acquired after patient positioning. The blurred diaphragm dome in CBCT was considered as the probability density function defining the range of liver motion. The liver contours from the planning CT were manually matched with CBCT to know the adequacy of IM. On the other hand, recently, the 4D CBCT verification imaging is also used for this purpose.^[57,58]

Respiratory gating

The motion-encompassing method includes large amount of normal tissues and hence it may not be an optimal approach. Techniques to include the respiratory motion with reduced margin are being developed. Gating is such a technique which administrates the radiation delivery at particular point of respiration [Figure 3] and results in reduced ITV margin. There are two types of gating techniques commonly employed; (a) phase gating and (b) amplitude gating. In the phase gating, the radiation beam is turned on whenever the respiratory signal is within the gating window that is defined based on respiratory signal phase [Figure 3a]. The amplitude gating is also referred as “displacement gating.” In this method, the radiation beam is turned on whenever the respiratory signal is within the gating window that is defined based on amplitude/displacement of the respiratory signal [Figure 3b].

Gating in radiotherapy is being studied since 1989 by various authors.^[59-64] A pioneer study about gating was carried out in early 1990 in Japan. Ohara *et al.*^[59] reported the first application of gating in a linear accelerator which uses a microwave oscillator to start/stop the radiation beam at particular point of respiration. Efficacy of gating technique was also tested in phantoms and it was also extended to patients. The respiratory motion was measured using an airbag system which was placed over patient. Tada *et al.*^[61] reported successful clinical implementation of gating techniques for the treatment of six lung cancer patients and observed that the gating requires longer time (double) than the conventional treatments. Since the radiation beam is delivered with multiple beam holds in gating technique, the beam characteristics should be verified, and various investigations compared the beam characteristics under gated operation with non-gated beam.^[62,63] One of the first studies evaluating the dosimetric characteristics of gated photon beams was reported by Ramsey

et al.^[62,63] Varian linear accelerator (Clinac 2100C/D) was used for the gated delivery of 6 MV and 18 MV X-ray photon beams. The beam output, energy, flatness, and symmetry deviations (compared to non-gated measurements) under gating were <0.8% in various gating duty cycles. They also emphasized that though the deviations of radiation beam under gating may be clinically insignificant, its performance should be evaluated and compared with non-gated operation before clinical implementation. Kubo *et al.*^[65] presented a complete workflow of breathing synchronized radiotherapy treatment starting from simulation, CT scan, treatment planning, and radiation treatment delivery. Their gating system consisted of a respiration monitoring system and linac with gating hardware and software. Fluoroscopy images synchronized with respiratory motion were recorded for defining the gating window. The respiratory signals could be used to gate the X-ray beam at appropriate gating window. The gating system was capable of performing both breath-hold and gating techniques.

In principle, gating can be delivered based on either phase or amplitude of respiratory motion. For a regular and periodic respiratory motion, both the amplitude and phase gating would result in similar (not identical) duty cycle and residual target motion. In case of irregular breathing, the amplitude gating may result in less residual error than phase gating, but the duty cycle (defines fraction of time during which the beam is “ON”) would be higher.^[66] The breath-hold is also another form of gating in which the radiation beam is administrated during breath-hold, and it requires a breath-hold CT for treatment planning. The main advantage of breath-hold is that the duty cycle is increased with minimal/no residual target motion, and the main disadvantage is that it may not be applicable to all lung cancer patients due to their pulmonary compromised status. The breath-hold technique may be a valuable technique in the left breast cancer radiotherapy for decreasing the cardiac complications, where the breath-hold can be used to push the chest wall away from the heart.^[67]

Optimizing the parameters related to gated treatment is very important for accurate radiation treatment delivery. Vedam *et al.*^[68] determined the optimal duty cycle that balances the treatment margin and time. They observed a phase shift between diaphragm and external chest wall motion, and it was up to 12% (42°) for a patient. Gating during exhale was more reproducible than inhale, and for a patient, they determined

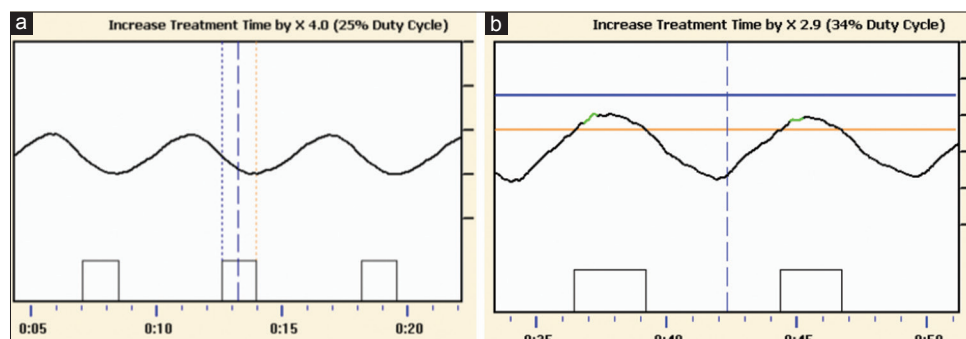


Figure 3: The gating treatment based on (a) phase and (b) amplitude

that 40% duty cycle was optimal. However, they also stated that these findings may differ from case to case and should be evaluated on an individual basis.

Respiratory gating is also extended for the dynamic treatments such as IMRT. Kubo and Wang^[69] tested the compatibility of Varian linac (2100C) for EDW and IMRT delivery under gated operation and observed no deviation. Similarly, the gating technique is also introduced in the arc treatments. Nicolini *et al.*^[70] investigated the feasibility of delivering the VMAT treatment by RapidArc under gated operation and concluded that the gating during RapidArc delivery was feasible. Recently, feasibility of gating during electron beam treatments has also been attempted.^[71]

To capture the patient's respiratory wave, additional devices are required. The respiratory wave can be generated using either external surrogates or internal tumor/surrogates and the gating based on these methods are referred to as "external gating" or "internal gating," respectively. Often, the gated delivery of lung tumor is based on the external surrogate signals because such systems are cost-effective and provide real-time signals without any ionizing radiation, and Figure 4 shows commercially available systems. The external surrogate signals can be derived using one of the following methods:

1. Measuring the abdominal pressure by strain gauges (Anzai respiratory gating system)
2. Measuring the chest wall motion by either optical system coupled with infrared (IR) source and camera (Varian RPM system) or laser surface imaging
3. Measuring the inspiration and expiration air volume using spirometry (Elekta ABC system) or temperature change.

However, the external surrogate motion may not accurately represent the internal tumor motion; there may be a phase

shift between external surrogate motion and the internal tumor motion which needs to be corrected or accounted (by correlation) during treatment simulation.^[1] Nevertheless, it was shown that phase shift observed between internal tumor motion and external surrogate motion during the simulation process was not constant over the course of radiotherapy treatment and there may be a phase offset.^[72-75]

Usually, the internal gating techniques require a fiducial marker implanted on/near to the target for tracking the respiratory motion. Smith *et al.*^[76] reported a successful implementation of gating technique using the real-time tumor motion signal (without the use of radiation dose for imaging) obtained from implanted wireless electromagnetic (EM) transponders. The latency (or delay) of transponders was within acceptable range and this resulted in better dosimetric accuracy during gated delivery. Insertion of fiducial marker through percutaneous method is associated with increased risk of pneumothorax. Therefore, bronchoscopic placement of marker with the assistance of multimodality imaging was also explored.^[77]

Alternatively, markerless tumor-tracking techniques are also being explored. Serpa *et al.*^[78] reported a gated treatment verification method using electronic portal imaging device (EPID) markerless tracking technique for the treatment of seven lung cancer patients. An integral part of their system was in-house developed software called portal track, and this tracks the target position in the EPID images without any fiducial marker. They demonstrated the feasibility of determining the tumor position using EPID images without using the fiducial markers during the gated treatment delivery.

The gating technique is indicated to the patients who have regular and reproducible respiration with the tumor motion >5 mm.^[1] The treatment verification imaging of gated treatment should also be under gated operation so that the time-dependent patient anatomy can be verified effectively.

One of the important issues during gated treatment is "trigger delay," and it is defined as the time delay between the gating trigger initiation from the respiratory device and the response (beam "ON") of the treatment unit. Improper characterization of time delay would result in positional errors in delivering the dose during gating, and this leads to missing of target or overdose of critical organs. Jin *et al.*^[79] presented a method to measure trigger delay of gating system using a simple motion phantom. They reported a value of 0.17 ± 0.03 s delay for linac-based gating system.

Finally, all the new technology development success relies on clinical results. Giraud *et al.*^[80] reported a multicenter study that compares respiratory gated conformal treatments and conventional conformal treatments and showed that the respiratory gating (breath-hold/gating) techniques could able to reduce the toxicities related to lungs, heart, and esophagus. It demonstrated that the theoretical/physical advantages of respiratory gating (breath-hold/gating) have correlation with clinical findings.

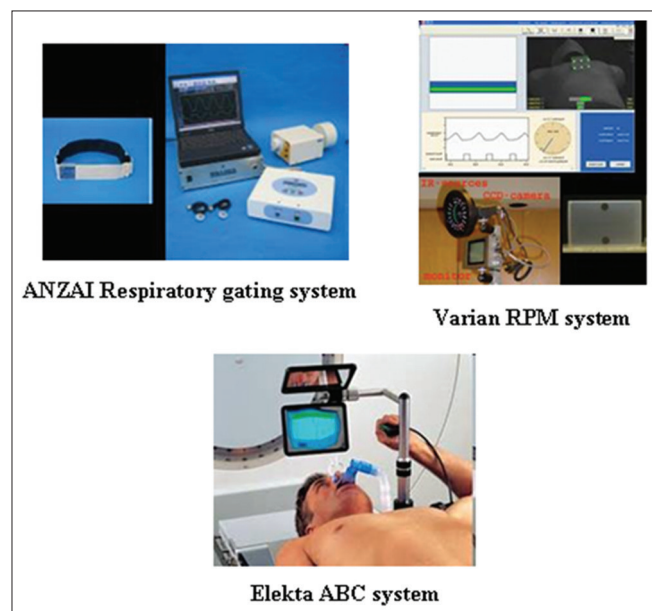


Figure 4: Commercially available external surrogate breathing monitoring systems used in gating

Real-time tumor tracking

Gating techniques prolong treatment time and this may increase patient discomfort and decreases patient throughput. Due to this, gating is not widely used in clinics. Technical developments with main focus on accounting respiration-induced motion without any beam-hold have resulted in real-time tumor-tracking techniques. Real-time tracking methods include two important processes as follows:

1. Real-time target position determination
2. Real-time beam adaptation.

Determining real-time target position

One of the important processes in real-time tracking is the determination of real-time target position, and there are various tools available such as MV imager,^[81] kV imager,^[82-84] stereoscopic imaging,^[85] hybrid systems,^[86] and EM transponders.^[87-91] Keall *et al.*^[81] developed a method based on EPID to track the target motion in real-time and evaluated this method using a dynamic thorax phantom which was implanted with three gold markers. Although they concluded that EPID-based tumor tracking is possible, there exists a latency period and it can be managed by motion prediction.

Poulsen *et al.*^[82-84] demonstrated a method to localize the moving target position in real time using a single kV imager. The moving target positions were captured using the kV fluoroscopic imaging during the arc delivery. They showed that this method was able to characterize the target motion within 2 mm geometrical accuracy. To add additional advantage, both MV and kV imagers were used to acquire the moving target position. Cho *et al.*^[92] developed a method for real-time target position using combined kV/MV imaging, and using this method, Dynamic Multi Leaf Collimator (DMLC)-based tracking deliveries were attempted in Varian Trilogy linac system. The dosimetric and geometric accuracy (<1 mm with prediction algorithm) was observed to be improved with this combined tracking system. However, the time delay of the integrated system was considerable (~450 ms) and this required the prediction of target position in advance.

kV and MV imaging utilizes ionizing radiation for imaging, and continuous imaging of patient for real-time target position would end up with large radiation dose to the patient. Therefore, techniques evolved to minimize/eliminate the ionizing radiation dose. One such method is the Synchrony system available with Cyberknife robotic tracking system which uses both IR camera (external surrogate) and kV stereoscopic imaging (internal surrogate) for moving target localization.^[86] Before the treatment delivery, a correlation is determined between IR and X-ray imaging system, and the treatment is continued with IR tracking alone. The validity of this correlation is continuously updated with frequent X-ray imaging.

Another way of eliminating imaging dose is to use non-ionizing radiations, and this is achieved with the EM transponder-based target tracking technique which uses implanted beacon transponders and EM array to monitor the real-time target movements. The Calypso system is the commercially available

EM tracking system which was successfully used for gated treatments, and also, recently, the system is extended for tracking techniques. Sawant *et al.*^[87] integrated the commercial Calypso system with a DMLC-based tracking system. The performance of the system in terms of latency (220 ms) and geometric accuracy (<2 mm) was promising. Similarly, Smith *et al.*^[88] also showed the feasibility of DMLC-based target tracking with Calypso system for IMRT delivery. In a follow-up study, Keall *et al.*^[89] used this system for the target tracking in intensity-modulated arc therapy delivery and demonstrated the advantage of this system in reducing the dosimetric uncertainties of target motion. Recently, MRI imaging integrated with linac has also been used to determine target motion in real time for DMLC tracking delivery.^[93]

Real-time beam adaptation

Various approaches such as robotic linac,^[94-97] couch movement,^[98-103] gimbaled linac,^[104-109] and dynamic MLC^[110-141] are available for the real-time tracking.

Tracking using robotic linac

First feasibility of tracking of respiration-induced target motion was achieved with Cyberknife[®] system which was developed by Schweikard *et al.*^[94,95] This system has a robotic arm which moves the linac to follow the moving target. Both the IR camera and X-ray imaging (implanted fiducial markers) are used to precisely locate the moving target position. Before the treatment delivery, a correlation is determined between IR and X-ray imaging system, and the validity of this correlation is continuously updated with frequent X-ray imaging. This robotic-based real-time tracking is clinically used for various sites such as lung, liver, and pancreas, and it is also extended for the tracking of respiration without implanted fiducials.^[96]

Winter *et al.*^[97] retrospectively analyzed (27 patients) the accuracy of Cyberknife system during robotic radiosurgery of liver using post-treatment log file record and reported the errors (3D radial error – mean \pm SD) such as, correlation errors (1.68 ± 1.13 mm), prediction errors (0.26 ± 0.13 mm), end-to-end tracking errors (0.57 ± 0.22 mm), and total errors (1.79 ± 1.16 mm). Among all the uncertainties, correlation errors were the major contributor and these errors were weakly related to target motion amplitude.

Couch-based tracking

Another solution for tracking the respiration-induced target motion is to use the treatment couch system. The couch-based tracking was first demonstrated by D'Souza *et al.*^[98] using a miniature adaptive couch model made up of two moving platforms which simulate the target motion as well as the table/couch movement, respectively. Both the platforms were connected together with an electronic feedback loop. Feasibility of this approach was tested in film measurements, and it was observed that the couch model (bottom platform) was able to follow the top platform motion. Further, they extended this model to a robotic couch, i.e., Hexapod[™] which was connected with an infrared camera for real-time tracking.

Unlike other tracking methods, the couch-based tracking has several limitations. In another study, D'Souza *et al.*^[99] theoretically evaluated the essential couch and controller dynamics for successful couch-tracking system. They determined that to obtain a residual motion <3 mm for the lung tumor motions used in their study, the couch motors with a maximum velocity 16.2 cm/s, 24 times increase in power, and a linear response with input steps up to 3 cm (relative to Hexapod™) were required. This showed that the control system feedback was greatly dependent on both the controller design and velocity/acceleration constraints. Similarly, Wilbert *et al.*^[100] also demonstrated the feasibility of tracking using Hexapod™ and also emphasized the importance of hardware improvement. They showed that the Hexapod™ couch was not able to track the target motion velocity >1 cm/s and they also observed a large latency of 400–500 ms for the image-based tracking with respiration periods of 4–5 s.

In addition to the technical limitation, patient comfort is another important concern for the clinical implementation of couch-based tracking. D'Souza *et al.*^[101] showed that patients over a moving couch did not experience motion sickness or external surface instability and this was also supported by Sweeney *et al.*^[102] Another challenge for couch-based tracking is the change in anatomical position (i.e., breathing amplitude variation) due to couch motion. Although D'Souza *et al.*^[101] observed no systemic variation between stationary and movement condition, Wilbert *et al.*^[103] observed lateral movement of the chest wall when couch moved in the craniocaudal and anterior-posterior direction.

Tracking using gimbaled system

The third approach for tracking the respiration-induced target motion uses gimbaled X-ray head. Kamino *et al.*^[104] developed a novel gimbaled X-ray head for 4D image-guided radiotherapy called Vero (collaborative development of BrainLAB AG, Feldkirchen, Germany and Mitsubishi Heavy Industries, Tokyo, Japan). The system has a 6 MV C-band linac and a MLC system attached to an O-ring gantry. The linac assembly is fitted to two orthogonal gimbals for pan and tilt motions of the X-ray beam, and this enables the possibility of real-time tracking of moving targets with independent DMLC motion for intensity modulation. The Vero system is also equipped with three imaging detectors; an EPID portal imaging device for MV imaging and two orthogonal kV imaging systems (attached with the O-ring at 45° from the central axis of MV beam). This system showed an excellent geometric accuracy (<1 mm) and system latency (<50 ms with IR camera tracking).^[105]

Recently, the Vero system was successfully implemented in clinical practice.^[106,107] Depuydt *et al.*^[106] reported first clinical experience with Vero tumor-tracking system. They observed that planning target volume (PTV) reduction due to tracking was 35% for single lesion SBRT and this translated to less lung and liver complication probability (1%). They also recommended to use a GTV-PTV margin of 5 mm and advised not to reduce the margin below 5 mm without proper understanding of biological

characteristics of tumor. Similarly, Iizuka *et al.*^[109] also reported their experience with Vero tumor-tracking system for liver SBRT treatment, and on average, the mean dose of the liver was reduced to 16% without compromising the tumor dose/tumor control (11-month median follow-up and 90% local control rate). The predictive errors of Vero tracking system for liver treatments were within couple of millimeters (95th percentiles: 1.1, 2.3, and 1.7 mm in the left-right, craniocaudal, and anterior-posterior directions, respectively).

Tracking using dynamic multileaf collimator

The last approach for tracking the respiration-induced target motion is based on DMLC whose motion is synchronized with the moving target. This approach was first proposed by Keall *et al.*^[110] who showed the feasibility of tracking in a DMLC-based IMRT delivery. Neicu *et al.*^[111] described synchronized moving aperture radiotherapy (SMART) in which the respiration-induced target motion was synchronized with the IMRT leaf motions. It was shown that the error during SMART could be kept to within couple of millimeters for 4 out of 11 lung motions with reasonable delivery efficiency under free breathing conditions.

Tracking in three-dimensional conformal radiation therapy (3DCRT) is relatively easy and straight forward, but the same in IMRT is a challenging task as the leaf motion of MLC should not only follow the respiration-induced target motion but also as required for intensity modulation. The usual leaf motion calculation algorithms (for 3D IMRT) are not adequate for tracking, and sophisticated algorithms are required. Extensive theoretical investigations for synchronizing the target motion (one-dimensional [1D]) during IMRT delivery were carried out by Papiez *et al.*^[112-116] and Webb *et al.*^[117-124]

Papiez^[112,113] developed algorithms to synchronize the prior rigid target motions during dynamic IMRT delivery; a leaf motion formulation was derived for delivering the IMRT to a 1D moving rigid target with two technical constraints (predefined IMRT fluence and maximum MLC leaf speed) with an emphasis to minimize the irradiation time (number of MUs). Later, the algorithm was extended to include the target deformation.^[114] The target deformation was simplified into a 1D translational motion of target center of mass due to expansion and compression of target, and this was inputted during MLC leaf sequencing. Similar to the previous rigid target algorithm, the two constraints were also included in the study. Webb^[117] investigated the effect of intrafractional target motion in IMRT delivery and suggested a practical strategy called “stretch-and-shift-the-planned-modulations” for incorporating the target motions. The density change due to respiration is also another issue, and the effect should be understood. Webb^[119] showed that the density change due to breathing is fairly small. Webb and Binnie^[120] demonstrated the feasibility of tracking differential target motion with deformation during IMRT and determined that mean position was the best method; in a follow-up study, McClelland *et al.*^[125] implemented this method in 4DCT.

The above algorithms were able to include only 1D motion (parallel to MLC leaf motion) whereas the target is moving in 3D. Rangaraj *et al.*^[126] developed an algorithm to track the 2D target motion (both parallel and perpendicular to MLC leaf motion) in IMRT. The target motion parallel to MLC leaf motion was accounted similar to previous algorithms, and the perpendicular target motion was accounted by translating the leaf positions from one leaf to the next that matches the target motion in that axis. To achieve optimal leaf shifting, the MLC leaf motions were synchronized using a mid-time trajectory. For a given leaf pair, the mid-time trajectory lies at middle of leading and trailing leaves trajectories.

Previously discussed algorithms considered only prior target motion which is suboptimal because the target motions measured at simulation may not be same/constant during treatment delivery; therefore, robust real-time algorithms are required. The above-discussed algorithms were also extended to include the real-time target motion.^[115,127]

Experimental investigations of tracking with a clinical linear accelerator were also attempted. McQuaid *et al.*^[128] demonstrated the feasibility of tracking a target motion during IMRT delivery using an Elekta linac with MLCi system. The experiments were carried out using a moving phantom programmed to reproduce 2D elliptical motion in BEV for the breathing period of 10 s. Results of this study showed that the tracking delivery was similar to static delivery and this ensured that the linac was capable for the tracking technique. One of the notable experimental works on tracking was reported by Sawant *et al.*^[129] who developed and demonstrated a novel 3D real-time tracking algorithm for 3DCRT, IMRT, and VMAT. The proposed algorithm was capable of obtaining real-time target motion from a separate motion monitoring system and reshape the MLC apertures as per the target motion. Preliminary studies involving the geometric (using an in-house DMLC tracking system) and dosimetric accuracy measurements (Varian Trilogy) showed promising results. The algorithm resulted in a submillimeter geometric accuracy and superior dosimetric accuracy (4.8, 1.7, 2.3, and 3.8 times dosimetric improvement in 3DCRT, step-shoot IMRT, dynamic IMRT, and VMAT). Tracking the perpendicular target motion (target motion perpendicular to MLC leaf motion; usually Y-axis motion [craniocaudal] when collimator is set to 0°) resulted in significantly less treatment efficiency compared to parallel tracking (target motion parallel to MLC leaf motion; usually X-axis motion [mediolateral] when collimator is set to 0°).

Tewatia *et al.*^[130] demonstrated a breathing synchronized delivery (BSD) for IMRT in a clinical linear accelerator without any hardware modifications. In this method, 1D target motion (parallel to MLC leaf motion) was overlaid with DMLC leaf motions. The average target motion trajectory was obtained by deformable image registration of 4DCT images. A key point in the BSD is the constancy of patient breathing, i.e., during treatment delivery patient should breathe similar

to 4DCT simulation. The feasibility of this technique was demonstrated in phantom experiments, and dosimetric results showed that the BSD could significantly reduce the target motion uncertainties. Tacke *et al.*^[131] designed a dynamic real-time MLC control system for Siemens 160 MLC™. This control system contains specialized algorithms for continuous reshaping of MLC aperture as per real-time target position. Experimental measurements were carried out to measure the dosimetric accuracy of the tracking system using Gafchromic films. It was observed that the tracking system improved the dosimetric accuracy (gamma evaluation pass rate [2%/2 mm]) from 19% to 77% for a clinical IMRT. However, the main limitations of the new tracking system were the latency (400 ms) and the MLC leaf width (5 mm). Breathing motion variation or irregularity is an important concern for tracking. For the patients who have irregular breathing, the audiovisual feedback system may be useful for regularizing the breathing pattern.^[132] Alternatively, other techniques can also be employed to handle the breathing irregularity. Yi *et al.*^[133] developed a novel method called dose rate-regulated tracking (DRRT) for real-time tumor tracking using DMLC with free breathing condition. The DRRT method used the preprogrammed DMLC leaf motions synchronized with prior target motions, and any variation/irregularity in breathing was handled with real-time dose rate modification. The dose rate modifications would either speed up or slow down the radiation delivery.

Fixed field IMRT has evolved to VMAT to achieve further dose conformity and treatment efficiency. Due to the increased clinical utility, almost all the new machines are coming up with VMAT capability. Recently, few studies attempted to accommodate respiration-induced target motion during VMAT treatments.^[134-137] Sun *et al.*^[135] proposed an optimal VMAT algorithm to track 2D rigid target motion in the BEV. The target motion along with DMLC leaf motion was included through MLC leaf velocity modification whereas the target motion perpendicular to MLC leaf motion was accommodated by shifting the MLC leaves appropriately.^[126]

Davies *et al.*^[136] evaluated the VMAT tracking using computer simulations. They reported that faster MLC leaf velocity is beneficial for larger velocity target motions; further, the tracking accuracy was observed to be improved with decreased control point spacing and was dependent on the target motion velocity. In a follow-up study, Davies *et al.*^[137] carried out experimental and simulation measurements with Elekta Agility MLC system for VMAT tracking. The dosimetric results were promising and they highlighted the advantage of Agility MLC in VMAT tracking. Zimmerman *et al.*^[138] attempted to track the respiration-induced target motion in Varian RapidArc™ delivery. Their results demonstrated that the DMLC tracking with RapidArc™ is feasible; however, they observed a difficulty due to the noise originating from the RPM system which influenced the tracking delivery.

The real-time tracking system has various technical constraints such as physical limitation of MLC leaf velocity

and acceleration and latency (delay), which should be characterized for optimal treatment delivery. The MLC leaf speed limitation is an important issue for DMLC tracking, especially when using leaf shifting strategy for 2D tracking. Wijesooriya *et al.*^[139] measured the maximum leaf speed and acceleration/deceleration (at dose rate 300 MU/min) of Varian Millennium 120 MLC system to determine whether the MLC system is capable of DMLC tracking. The maximum MLC leaf speed was observed to be 3.3–3.9 cm/s at isocenter whereas the acceleration and deceleration were 50–69 cm/s² and 46–52 cm/s², respectively. They concluded that the MLC characteristics were suitable for DMLC tracking for up to 97% of respiration, and during the use of larger velocities, the beam should be temporarily stopped (beam-hold). Rangaraj *et al.*^[126] evaluated the impact of MLC leaf speed limitation on DMLC tracking of 2D target motion and concluded that the dosimetric errors were completely eliminated when the leaf speed limitation is removed.

The latency (delay) of tracking system would create a misalignment between the radiation beam and moving target.^[142-146] Therefore, this should be thoroughly measured for a tracking system and should be accounted for. Table 3 shows the latency period of different tracking techniques. Poulsen *et al.*^[143] developed a method to analyze the latency period of a prototype image-based DMLC tracking system. They reported a latency period of 380 ± 9 ms and 420 ± 12 ms for MV and kV image-based tracking, respectively, when using the image acquisition interval 150 ms. Webb *et al.*^[121] also developed a theoretical model to quantify the uncertainties due to latency of DMLC tracking system and concluded that the uncertainties of system latency depend on the intensity modulation, changes in breathing condition, and the magnitude of latency period. Recently, Bedford *et al.*^[146] investigated the dosimetric effect of latency on the DMLC-based tracking in VMAT for five SBRT lung patients. The latency was changed from 0 to 500 ms with 50 ms steps. They demonstrated that the latency period <150 ms resulted in minor effect on the VMAT tracking and the latency period >150 ms definitely requires a margin.

Recently, the DMLC-based has been implemented clinically. Keall *et al.*^[91] reported the first clinical treatment of a prostate patient using EM transponder-guided (Calypso) DMLC tracking and observed a decreased rectal dose (for an average shift 1.2 mm) with DMLC tracking compared to non-tracking. Same group^[147] also extended the DMLC tracking for lung stereotactic ablative body radiotherapy. Compared to standard ITV approach, DMLC tracking reduced the PTV volume by 41% and the lung dose was also decreased (51% mean lung dose; 51% lung V20 and 51% lung V5).

SUMMARY

Respiration facilitates tumors such as lung, liver, kidney, pancreas, esophagus, and prostate to be dynamic, and the majority of motion is observed to be in the craniocaudal direction. Small size lung tumors attached to lower lobe are

Table 3: Latency of different real-time tracking methods

Author (s)	Tracking system	Latency (ms)
Sawant <i>et al.</i> ^[87]	Millennium 120 MLC + Calypso	~220
Depuydt <i>et al.</i> ^[105]	Vero+ExacTrac	47.7
Tacke <i>et al.</i> ^[131]	Siemens 160 MLC™	400.0
Keall <i>et al.</i> ^[142]	Millennium 120 MLC + RPM system	160.0
Poulsen <i>et al.</i> ^[143]	Millennium 120 MLC + MV imager (AS1000)	380.0±9.0
	Millennium 120 MLC + kV imager (OBI)	420.0±12.0
Hoogeman <i>et al.</i> ^[144]	Cyberknife + Synchrony	192.5
Fast <i>et al.</i> ^[145]	Agility MLC	37-69

MLC: Multileaf collimator, OBI: Onboard imager

observed to move more compared to large size tumors attached to the middle and upper lobe.

Respiration-induced target motion affects all the processes of radiation therapy. During treatment delivery, respiratory motion introduces dosimetric uncertainties. In case of non-dynamic treatment delivery, respiratory motion produces averaging and blurring of dose at field edge, whereas in dynamic treatment delivery, it also produces interplay effect which is created due to the simultaneous motion of MLC leaves and target. It has been shown that the dosimetric impact of respiratory motion is averaged out in conventional fractionation as well as hypofractionation treatments, i.e., SBRT.

Three ways of managing respiratory motion are reported, i.e., (1) motion-encompassing method, (2) gating, and (3) tracking.

In motion-encompassing method, treatment field aperture is opened wide enough to include entire target motion trajectory. Various approaches were reported to determine the target motion trajectory (or ITV), i.e., fluoroscopy, slow CT, breath-hold CT, 4DCT, CBCT, etc., Among all, 4DCT is considered to be standard of care for defining ITV. However, respiration-induced target motion observed during simulation may not be constant, and there may be an interfractional variation which should be considered while defining the margins.

In gating, as treatment is delivered during particular time/phase of respiration, resultant ITV volume is relatively small compared to motion-encompassing method, whereas the treatment time is prolonged. Since gating requires multiple beam interruptions/beam-hold, the dosimetric characteristics (beam output, flatness, and symmetry) of gated delivery should be compared and verified against the corresponding non-gating delivery. Gating during exhale is observed to be more reproducible. Gated technique can also be used during dynamic treatments such as IMRT and VMAT. Trigger delay in a gated delivery should be measured and accounted for accurate targeting. Any phase shift between the internal target motion and external surrogate motion should be measured and included while planning gated delivery. In addition, constancy of respiratory motion and phase shift (between the internal

target motion and external surrogate motion) over the course of treatment should also be monitored. The breath-hold is also another form of gating in which the radiation beam is administered during breath-hold. Breath-hold is advantageous because it increases duty cycle with minimal/no residual target motion whereas the main disadvantage is that it may not be applicable to all lung cancer patients due to their pulmonary compromised status. The breath-hold technique may be a valuable technique in the left breast cancer radiotherapy for decreasing the cardiac complications, where the breath-hold can be used to push the chest wall away from the heart.

Gating technique prolongs treatment time and this may cause patient discomfort and decrease patient throughput. In tracking technique, treatment is delivered without any beam hold. In principle, tracking can be achieved through the motion of either robotic linac or couch or linac attached with gimbaled mechanism or dynamic MLC. Tracking using robotic linac and gimbaled mechanism is commercially available in Cyberknife robotic system (Accuray, Sunnyvale, CA) and Vero system (BrainLAB AG, Feldkirchen, Germany) respectively, and the DMMLC-based tracking has been recently implemented in clinical practice. DMMLC-based tracking has several technical limitations, i.e., maximum velocity, acceleration/deceleration of leaves, etc., that should be addressed before clinical implementation. To circumvent imaging dose, alternative methods such as hybrid techniques (external surrogate signal using optical system plus internal target motion using X-ray imaging), EM transponders, and MRI are being explored to determine real-time target position. All tracking methods have inevitable latency period which is defined as the time delay between target position and tracking system response. It was observed that latency period <150 ms would not affect the delivery accuracy of tracking based on DMMLC.

This article appraises the current knowledge about the magnitude, uncertainties, and solutions of respiration-induced target motion, and it will be particularly helpful to the medical physicists and physicians for a better understanding of the respiratory motion management in radiation oncology.

Financial support and sponsorship

Nil.

Conflicts of interest

There are no conflicts of interest.

REFERENCES

- Keall PJ, Mageras GS, Balter JM, Emery RS, Forster KM, Jiang SB, *et al.* The management of respiratory motion in radiation oncology report of AAPM task group 76. *Med Phys* 2006;33:3874-900.
- SEER Cancer Statistics Factsheets: Lung and Bronchus Cancer. National Cancer Institute. Bethesda, MD. Available from: <http://www.seer.cancer.gov/statfacts/html/lungb.html>. [last assessed on 2017 Aug 27].
- Okunieff P, Morgan D, Niemierko A, Suit HD. Radiation dose-response of human tumors. *Int J Radiat Oncol Biol Phys* 1995;32:1227-37.
- Martel MK, Ten Haken RK, Hazuka MB, Kessler ML, Strawderman M, Turrisi AT, *et al.* Estimation of tumor control probability model parameters from 3-D dose distributions of non-small cell lung cancer patients. *Lung Cancer* 1999;24:31-7.
- Timmerman R, Paulus R, Galvin J, Michalski J, Straube W, Bradley J, *et al.* Stereotactic body radiation therapy for inoperable early stage lung cancer. *JAMA* 2010;303:1070-6.
- Timmerman R, Galvin J, Michalski J, Straube W, Ibbott G, Martin E, *et al.* Accreditation and quality assurance for radiation therapy oncology group: Multicenter clinical trials using stereotactic body radiation therapy in lung cancer. *Acta Oncol* 2006;45:779-86.
- ICRU Report 62. International Commission on Radiation Units and Measurements. Prescribing, Recording, and Reporting Photon Beam Therapy, Supplement to ICRU Report No. 50. Bethesda, MD: ICRU; 1999.
- Seppenwoolde Y, Shirato H, Kitamura K, Shimizu S, van Herk M, Lebesque JV, *et al.* Precise and real-time measurement of 3D tumor motion in lung due to breathing and heartbeat, measured during radiotherapy. *Int J Radiat Oncol Biol Phys* 2003;53:822-34.
- Shimizu S, Shirato H, Ogura S, Akita-Dosaka H, Kitamura K, Nishioka T, *et al.* Detection of lung tumor movement in real-time tumor-tracking radiotherapy. *Int J Radiat Oncol Biol Phys* 2001;51:304-10.
- Chen QS, Weinhaus MS, Deibel FC, Ciezki JP, Macklis RM. Fluoroscopic study of tumor motion due to breathing: Facilitating precise radiation therapy for lung cancer patients. *Med Phys* 2001;28:1850-6.
- Sixel KE, Ruschin M, Tirona R, Cheung PC. Digital fluoroscopy to quantify lung tumor motion: Potential for patient-specific planning target volumes. *Int J Radiat Oncol Biol Phys* 2003;57:717-23.
- Yu ZH, Lin SH, Balter P, Zhang L, Dong L. A comparison of tumor motion characteristics between early stage and locally advanced stage lung cancers. *Radiother Oncol* 2012;104:33-8.
- Plathow C, Ley S, Fink C, Puderbach M, Hosch W, Schmähle A, *et al.* Analysis of intrathoracic tumor mobility during whole breathing cycle by dynamic MRI. *Int J Radiat Oncol Biol Phys* 2004;59:952-9.
- Mageras GS, Pevsner A, Yorke ED, Rosenzweig KE, Ford EC, Hertanto A, *et al.* Measurement of lung tumor motion using respiration-correlated CT. *Int J Radiat Oncol Biol Phys* 2004;60:933-41.
- Lever FM, Lips IM, Crijns SP, Reerink O, van Lier AL, Moerland MA, *et al.* Quantification of esophageal tumor motion on cine-magnetic resonance imaging. *Int J Radiat Oncol Biol Phys* 2014;88:419-24.
- Patel AA, Wolfgang JA, Niemierko A, Hong TS, Yock T, Choi NC, *et al.* Implications of respiratory motion as measured by four-dimensional computed tomography for radiation treatment planning of esophageal cancer. *Int J Radiat Oncol Biol Phys* 2009;74:290-6.
- Brix L, Ringgaard S, Sørensen TS, Poulsen PR. Three-dimensional liver motion tracking using real-time two-dimensional MRI. *Med Phys* 2014;41:042302.
- Park JC, Park SH, Kim JH, Yoon SM, Song SY, Liu Z, *et al.* Liver motion during cone beam computed tomography guided stereotactic body radiation therapy. *Med Phys* 2012;39:6431-42.
- Feng M, Balter JM, Normolle D, Adusumilli S, Cao Y, Chenevert TL, *et al.* Characterization of pancreatic tumor motion using cine MRI: Surrogates for tumor position should be used with caution. *Int J Radiat Oncol Biol Phys* 2009;74:884-91.
- Goldstein SD, Ford EC, Duhon M, McNutt T, Wong J, Herman JM, *et al.* Use of respiratory-correlated four-dimensional computed tomography to determine acceptable treatment margins for locally advanced pancreatic adenocarcinoma. *Int J Radiat Oncol Biol Phys* 2010;76:597-602.
- Knybel L, Cvek J, Otahal B, Jonszta T, Molenda L, Czerny D, *et al.* The analysis of respiration-induced pancreatic tumor motion based on reference measurement. *Radiat Oncol* 2014;9:192.
- Yamashita H, Yamashita M, Futaguchi M, Takenaka R, Shibata S, Yamamoto K, *et al.* Individually wide range of renal motion evaluated by four-dimensional computed tomography. *Springerplus* 2014;3:131.
- Abhilash RH, Chauhan S, Che MV, Ooi CC, Bakar RA, Lo RH, *et al.* Quantitative study on the effect of abnormalities on respiration-induced kidney movement. *Ultrasound Med Biol* 2016;42:1681-8.
- Pham D, Kron T, Foroudi F, Schneider M, Siva S. A review of kidney

- motion under free, deep and forced-shallow breathing conditions: Implications for stereotactic ablative body radiotherapy treatment. *Technol Cancer Res Treat* 2014;13:315-23.
25. Malone S, Crook JM, Kendal WS, Szanto J. Respiratory-induced prostate motion: Quantification and characterization. *Int J Radiat Oncol Biol Phys* 2000;48:105-9.
 26. Dinkel J, Thieke C, Plathow C, Zamecnik P, Prüm H, Huber PE, *et al.* Respiratory-induced prostate motion: Characterization and quantification in dynamic MRI. *Strahlenther Onkol* 2011;187:426-32.
 27. Erridge SC, Seppenwoolde Y, Muller SH, van Herk M, De Jaeger K, Belderbos JS, *et al.* Portal imaging to assess set-up errors, tumor motion and tumor shrinkage during conformal radiotherapy of non-small cell lung cancer. *Radiother Oncol* 2003;66:75-85.
 28. Maria Das KJ, Agarwal A, Yoganathan SA, Gowtham Raj D, Kumar S. Investigation of inter and intra-fractional uncertainties in lung IMRT delivery. *Int Fed Med Biol Eng* 2012;39:1857-9.
 29. Yu CX, Jaffray DA, Wong JW. The effects of intra-fraction organ motion on the delivery of dynamic intensity modulation. *Phys Med Biol* 1998;43:91-104.
 30. Pemler P, Besserer J, Lombriser N, Pescia R, Schneider U. Influence of respiration-induced organ motion on dose distributions in treatments using enhanced dynamic wedges. *Med Phys* 2001;28:2234-40.
 31. Bortfeld T, Jokivarsi K, Goitein M, Kung J, Jiang SB. Effects of intra-fraction motion on IMRT dose delivery: Statistical analysis and simulation. *Phys Med Biol* 2002;47:2203-20.
 32. Jiang SB, Pope C, Al Jarrah KM, Kung JH, Bortfeld T, Chen GT, *et al.* An experimental investigation on intra-fractional organ motion effects in lung IMRT treatments. *Phys Med Biol* 2003;48:1773-84.
 33. Li X, Yang Y, Li T, Fallon K, Heron DE, Huq MS, *et al.* Dosimetric effect of respiratory motion on volumetric-modulated arc therapy-based lung SBRT treatment delivered by trueBeam machine with flattening filter-free beam. *J Appl Clin Med Phys* 2013;14:4370.
 34. Ong C, Verbakel WF, Cuijpers JP, Slotman BJ, Senan S. Dosimetric impact of interplay effect on rapidArc lung stereotactic treatment delivery. *Int J Radiat Oncol Biol Phys* 2011;79:305-11.
 35. Stambaugh C, Nelms BE, Dilling T, Stevens C, Latifi K, Zhang G, *et al.* Experimentally studied dynamic dose interplay does not meaningfully affect target dose in VMAT SBRT lung treatments. *Med Phys* 2013;40:091710.
 36. Rao M, Wu J, Cao D, Wong T, Mehta V, Shepard D, *et al.* Dosimetric impact of breathing motion in lung stereotactic body radiotherapy treatment using intensity modulated radiotherapy and volumetric modulated arc therapy [corrected]. *Int J Radiat Oncol Biol Phys* 2012;83:e251-6.
 37. Mutaf YD, Scicutella CJ, Michalski D, Fallon K, Brandner ED, Bednarz G, *et al.* A simulation study of irregular respiratory motion and its dosimetric impact on lung tumors. *Phys Med Biol* 2011;56:845-59.
 38. Sidhu S, Sidhu NP, Lapointe C, Gryschuk G. The effects of intrafraction motion on dose homogeneity in a breast phantom with physical wedges, enhanced dynamic wedges, and ssIMRT. *Int J Radiat Oncol Biol Phys* 2006;66:64-75.
 39. Ikeda I, Mizowaki T, Ono T, Yamada M, Nakamura M, Monzen H, *et al.* Effect of intrafractional prostate motion on simultaneous boost intensity-modulated radiotherapy to the prostate: A simulation study based on intrafractional motion in the prone position. *Med Dosim* 2015;40:325-32.
 40. Berbeco RI, Pope CJ, Jiang SB. Measurement of the interplay effect in lung IMRT treatment using EDR2 films. *J Appl Clin Med Phys* 2006;7:33-42.
 41. Mohn S, Wasbø E. Simulation of respiratory motion during IMRT dose delivery. *Acta Oncol* 2011;50:935-43.
 42. Yoganathan SA, Maria Das KJ, Kumar S. Computational model to simulate the interplay effect in dynamic IMRT delivery. *Int J Phys Conf Serv* 2014;489:12042-7.
 43. Yoganathan SA, Maria Das KJ, Shiva Subramanian V, Raj DG, Agarwal A, Kumar S. Investigating different CT techniques for internal target volume definition. *J Cancer Res Ther* 2016; [Ahead of print].
 44. Lagerwaard FJ, Van Sornsen de Koste JR, Nijssen-Visser MR, Schuchhard-Schipper RH, Oei SS, Munne A, *et al.* Multiple "slow" CT scans for incorporating lung tumor mobility in radiotherapy planning. *Int J Radiat Oncol Biol Phys* 2001;51:932-7.
 45. Wurstbauer K, Deutschmann H, Kopp P, Sedlmayer F. Radiotherapy planning for lung cancer: Slow CTs allow the drawing of tighter margins. *Radiother Oncol* 2005;75:165-70.
 46. Shih HA, Jiang SB, Aljarrah KM, Doppke KP, Choi NC. Internal target volume determined with expansion margins beyond composite gross tumor volume in three-dimensional conformal radiotherapy for lung cancer. *Int J Radiat Oncol Biol Phys* 2004;60:613-22.
 47. Underberg RW, Lagerwaard FJ, Cuijpers JP, Slotman BJ, van Sörnsen de Koste JR, Senan S, *et al.* Four-dimensional CT scans for treatment planning in stereotactic radiotherapy for stage I lung cancer. *Int J Radiat Oncol Biol Phys* 2004;60:1283-90.
 48. Underberg RW, Lagerwaard FJ, Slotman BJ, Cuijpers JP, Senan S. Use of maximum intensity projections (MIP) for target volume generation in 4DCT scans for lung cancer. *Int J Radiat Oncol Biol Phys* 2005;63:253-60.
 49. Wang L, Hayes S, Paskalev K, Jin L, Buyyounouski MK, Ma CC, *et al.* Dosimetric comparison of stereotactic body radiotherapy using 4D CT and multiphase CT images for treatment planning of lung cancer: Evaluation of the impact on daily dose coverage. *Radiother Oncol* 2009;91:314-24.
 50. Wang Z, Wu QJ, Marks LB, Larrier N, Yin FF. Cone-beam CT localization of internal target volumes for stereotactic body radiotherapy of lung lesions. *Int J Radiat Oncol Biol Phys* 2007;69:1618-24.
 51. Wang L, Chen X, Lin MH, Xue J, Lin T, Fan J, *et al.* Evaluation of the cone beam CT for internal target volume localization in lung stereotactic radiotherapy in comparison with 4D MIP images. *Med Phys* 2013;40:111709.
 52. Chang G, Chang T, Pan T, Clark JW, Mawlawi OR. Determination of internal target volume from a single positron emission tomography/computed tomography scan in lung cancer. *Int J Radiat Oncol Biol Phys* 2012;83:459-66.
 53. Callahan J, Kron T, Schneider-Kolsky M, Dunn L, Thompson M, Siva S, *et al.* Validation of a 4D-PET maximum intensity projection for delineation of an internal target volume. *Int J Radiat Oncol Biol Phys* 2013;86:749-54.
 54. Guckenberger M, Wilbert J, Meyer J, Baier K, Richter A, Flentje M, *et al.* Is a single respiratory correlated 4D-CT study sufficient for evaluation of breathing motion? *Int J Radiat Oncol Biol Phys* 2007;67:1352-9.
 55. Britton KR, Starkschall G, Liu H, Chang JY, Bilton S, Ezhil M, *et al.* Consequences of anatomic changes and respiratory motion on radiation dose distributions in conformal radiotherapy for locally advanced non-small-cell lung cancer. *Int J Radiat Oncol Biol Phys* 2009;73:94-102.
 56. Guckenberger M, Sweeney RA, Wilbert J, Krieger T, Richter A, Baier K, *et al.* Image-guided radiotherapy for liver cancer using respiratory-correlated computed tomography and cone-beam computed tomography. *Int J Radiat Oncol Biol Phys* 2008;71:297-304.
 57. Yoganathan SA, Maria Das KJ, Mohamed Ali S, Agarwal A, Mishra SP, Kumar S, *et al.* Evaluating the four-dimensional cone beam computed tomography with varying gantry rotation speed. *Br J Radiol* 2016;89:20150870.
 58. Takahashi W, Yamashita H, Kida S, Masutani Y, Sakumi A, Ohtomo K, *et al.* Verification of planning target volume settings in volumetric modulated arc therapy for stereotactic body radiation therapy by using in-treatment 4-dimensional cone beam computed tomography. *Int J Radiat Oncol Biol Phys* 2013;86:426-31.
 59. Ohara K, Okumura T, Akisada M, Inada T, Mori T, Yokota H, *et al.* Irradiation synchronized with respiration gate. *Int J Radiat Oncol Biol Phys* 1989;17:853-7.
 60. Kubo HD, Hill BC. Respiration gated radiotherapy treatment: A technical study. *Phys Med Biol* 1996;41:83-91.
 61. Tada T, Minakuchi K, Fujioka T, Sakurai M, Koda M, Kawase I, *et al.* Lung cancer: Intermittent irradiation synchronized with respiratory motion – Results of a pilot study. *Radiology* 1998;207:779-83.
 62. Ramsey CR, Scapertho D, Arwood D, Oliver AL. Clinical efficacy of respiratory gated conformal radiation therapy. *Med Dosim* 1999;24:115-9.
 63. Ramsey CR, Cordrey IL, Oliver AL. A comparison of beam characteristics

- for gated and nongated clinical x-ray beams. *Med Phys* 1999;26:2086-91.
64. Hara R, Itami J, Kondo T, Aruga T, Abe Y, Ito M, *et al.* Stereotactic single high dose irradiation of lung tumors under respiratory gating. *Radiother Oncol* 2002;63:159-63.
 65. Kubo HD, Len PM, Minohara S, Mostafavi H. Breathing-synchronized radiotherapy program at the University of California Davis Cancer Center. *Med Phys* 2000;27:346-53.
 66. Murphy MJ. *Adaptive Motion Compensation in Radiotherapy*. Boca Raton, FL: CRC Press; 2012.
 67. Latty D, Stuart KE, Wang W, Ahern V. Review of deep inspiration breath-hold techniques for the treatment of breast cancer. *J Med Radiat Sci* 2015;62:74-81.
 68. Vedam SS, Keall PJ, Kini VR, Mohan R. Determining parameters for respiration-gated radiotherapy. *Med Phys* 2001;28:2139-46.
 69. Kubo HD, Wang L. Compatibility of varian 2100C gated operations with enhanced dynamic wedge and IMRT dose delivery. *Med Phys* 2000;27:1732-8.
 70. Nicolini G, Vanetti E, Clivio A, Fogliata A, Cozzi L. Pre-clinical evaluation of respiratory-gated delivery of volumetric modulated arc therapy with rapidArc. *Phys Med Biol* 2010;55:N347-57.
 71. Yoganathan SA, Maria Das KJ, Raj DG, Kumar S. Dosimetric verification of gated delivery of electron beams using a 2D ion chamber array. *J Med Phys* 2015;40:68-73.
 72. Hoisak JD, Sixel KE, Tirona R, Cheung PC, Pignol JP. Correlation of lung tumor motion with external surrogate indicators of respiration. *Int J Radiat Oncol Biol Phys* 2004;60:1298-306.
 73. Korreman SS, Juhler-Nøttrup T, Boyer AL. Respiratory gated beam delivery cannot facilitate margin reduction, unless combined with respiratory correlated image guidance. *Radiother Oncol* 2008;86:61-8.
 74. Redmond KJ, Song DY, Fox JL, Zhou J, Rosenzweig CN, Ford E, *et al.* Respiratory motion changes of lung tumors over the course of radiation therapy based on respiration-correlated four-dimensional computed tomography scans. *Int J Radiat Oncol Biol Phys* 2009;75:1605-12.
 75. Ionascu D, Jiang SB, Nishioka S, Shirato H, Berbeco RL. Internal-external correlation investigations of respiratory induced motion of lung tumors. *Med Phys* 2007;34:3893-903.
 76. Smith RL, Lechleiter K, Malinowski K, Shepard DM, Housley DJ, Afghani M, *et al.* Evaluation of linear accelerator gating with real-time electromagnetic tracking. *Int J Radiat Oncol Biol Phys* 2009;74:920-7.
 77. Steinfurt DP, Siva S, Kron T, Chee RR, Ruben JD, Ball DL, *et al.* Multimodality guidance for accurate bronchoscopic insertion of fiducial markers. *J Thorac Oncol* 2015;10:324-30.
 78. Serpa M, Baier K, Cremers F, Guckenberger M, Meyer J. Suitability of markerless EPID tracking for tumor position verification in gated radiotherapy. *Med Phys* 2014;41:031702.
 79. Jin JY, Yin FF. Time delay measurement for linac based treatment delivery in synchronized respiratory gating radiotherapy. *Med Phys* 2005;32:1293-6.
 80. Giraud P, Morvan E, Claude L, Mornex F, Le Pechoux C, Bachaud JM, *et al.* Respiratory gating techniques for optimization of lung cancer radiotherapy. *J Thorac Oncol* 2011;6:2058-68.
 81. Keall PJ, Todor AD, Vedam SS, Bartee CL, Siebers JV, Kini VR, *et al.* On the use of EPID-based implanted marker tracking for 4D radiotherapy. *Med Phys* 2004;31:3492-9.
 82. Poulsen PR, Cho B, Sawant A, Keall PJ. Implementation of a new method for dynamic multileaf collimator tracking of prostate motion in arc radiotherapy using a single kV imager. *Int J Radiat Oncol Biol Phys* 2010;76:914-23.
 83. Poulsen PR, Cho B, Sawant A, Ruan D, Keall PJ. Dynamic MLC tracking of moving targets with a single kV imager for 3D conformal and IMRT treatments. *Acta Oncol* 2010;49:1092-100.
 84. Poulsen PR, Cho B, Ruan D, Sawant A, Keall PJ. Dynamic multileaf collimator tracking of respiratory target motion based on a single kilovoltage imager during arc radiotherapy. *Int J Radiat Oncol Biol Phys* 2010;77:600-7.
 85. Takayama K, Mizowaki T, Kokubo M, Kawada N, Nakayama H, Narita Y, *et al.* Initial validations for pursuing irradiation using a gimbal tracking system. *Radiother Oncol* 2009;93:45-9.
 86. Ozhasoglu C, Saw CB, Chen H, Burton S, Komanduri K, Yue NJ, *et al.* Synchrony – Cyberknife respiratory compensation technology. *Med Dosim* 2008;33:117-23.
 87. Sawant A, Smith RL, Venkat RB, Santanam L, Cho B, Poulsen P, *et al.* Toward submillimeter accuracy in the management of intrafraction motion: The integration of real-time internal position monitoring and multileaf collimator target tracking. *Int J Radiat Oncol Biol Phys* 2009;74:575-82.
 88. Smith RL, Sawant A, Santanam L, Venkat RB, Newell LJ, Cho BC, *et al.* Integration of real-time internal electromagnetic position monitoring coupled with dynamic multileaf collimator tracking: An intensity-modulated radiation therapy feasibility study. *Int J Radiat Oncol Biol Phys* 2009;74:868-75.
 89. Keall PJ, Sawant A, Cho B, Ruan D, Wu J, Poulsen P, *et al.* Electromagnetic-guided dynamic multileaf collimator tracking enables motion management for intensity-modulated arc therapy. *Int J Radiat Oncol Biol Phys* 2011;79:312-20.
 90. Krauss A, Nill S, Tacke M, Oelfke U. Electromagnetic real-time tumor position monitoring and dynamic multileaf collimator tracking using a siemens 160 MLC: Geometric and dosimetric accuracy of an integrated system. *Int J Radiat Oncol Biol Phys* 2011;79:579-87.
 91. Keall PJ, Colvill E, O'Brien R, Ng JA, Poulsen PR, Eade T, *et al.* The first clinical implementation of electromagnetic transponder-guided MLC tracking. *Med Phys* 2014;41:020702.
 92. Cho B, Poulsen PR, Sloutsky A, Sawant A, Keall PJ. First demonstration of combined kV/MV image-guided real-time dynamic multileaf-collimator target tracking. *Int J Radiat Oncol Biol Phys* 2009;74:859-67.
 93. Crijns SP, Raaymakers BW, Lagendijk JJ. Proof of concept of MRI-guided tracked radiation delivery: Tracking one-dimensional motion. *Phys Med Biol* 2012;57:7863-72.
 94. Schweikard A, Glosser G, Bodduluri M, Murphy MJ, Adler JR. Robotic motion compensation for respiratory movement during radiosurgery. *Comput Aided Surg* 2000;5:263-77.
 95. Schweikard A, Shiomi H, Adler J. Respiration tracking in radiosurgery. *Med Phys* 2004;31:2738-41.
 96. Schweikard A, Shiomi H, Adler J. Respiration tracking in radiosurgery without fiducials. *Int J Med Robot* 2005;1:19-27.
 97. Winter JD, Wong R, Swaminath A, Chow T. Accuracy of robotic radiosurgical liver treatment throughout the respiratory cycle. *Int J Radiat Oncol Biol Phys* 2015;93:916-24.
 98. D'Souza WD, Naqvi SA, Yu CX. Real-time intra-fraction-motion tracking using the treatment couch: A feasibility study. *Phys Med Biol* 2005;50:4021-33.
 99. D'Souza WD, McAvoy TJ. An analysis of the treatment couch and control system dynamics for respiration-induced motion compensation. *Med Phys* 2006;33:4701-9.
 100. Wilbert J, Meyer J, Baier K, Guckenberger M, Herrmann C, Heß R, *et al.* Tumor tracking and motion compensation with an adaptive tumor tracking system (ATTS): System description and prototype testing. *Med Phys* 2008;35:3911-21.
 101. D'Souza WD, Malinowski KT, Van Liew S, D'Souza G, Asbury K, McAvoy TJ, *et al.* Investigation of motion sickness and inertial stability on a moving couch for intra-fraction motion compensation. *Acta Oncol* 2009;48:1198-203.
 102. Sweeney RA, Arnold W, Steixner E, Nevinny-Stickel M, Lukas P. Compensating for tumor motion by a 6-degree-of-freedom treatment couch: Is patient tolerance an issue? *Int J Radiat Oncol Biol Phys* 2009;74:168-71.
 103. Wilbert J, Baier K, Richter A, Herrmann C, Ma L, Flentje M, *et al.* Influence of continuous table motion on patient breathing patterns. *Int J Radiat Oncol Biol Phys* 2010;77:622-9.
 104. Kamino Y, Takayama K, Kokubo M, Narita Y, Hirai E, Kawawada N, *et al.* Development of a four-dimensional image-guided radiotherapy system with a gimbaled X-ray head. *Int J Radiat Oncol Biol Phys* 2006;66:271-8.
 105. Depuydt T, Verellen D, Haas O, Gevaert T, Linthout N, Duchateau M, *et al.* Geometric accuracy of a novel gimbal based radiation therapy tumor tracking system. *Radiother Oncol* 2011;98:365-72.
 106. Depuydt T, Poels K, Verellen D, Engels B, Collen C, Buleteanu M, *et al.* Treating patients with real-time tumor tracking using the vero gimbaled linac system: Implementation and first review. *Radiother*

- Oncol 2014;112:343-51.
107. Matsuo Y, Ueki N, Takayama K, Nakamura M, Miyabe Y, Ishihara Y, *et al.* Evaluation of dynamic tumour tracking radiotherapy with real-time monitoring for lung tumours using a gimbal mounted linac. *Radiother Oncol* 2014;112:360-4.
 108. Solberg TD, Medin PM, Ramirez E, Ding C, Foster RD, Yordy J, *et al.* Commissioning and initial stereotactic ablative radiotherapy experience with vero. *J Appl Clin Med Phys* 2014;15:4685.
 109. Iizuka Y, Matsuo Y, Ishihara Y, Akimoto M, Tanabe H, Takayama K, *et al.* Dynamic tumor-tracking radiotherapy with real-time monitoring for liver tumors using a gimbal mounted linac. *Radiother Oncol* 2015;117:496-500.
 110. Keall PJ, Kini VR, Vedam SS, Mohan R. Motion adaptive x-ray therapy: A feasibility study. *Phys Med Biol* 2001;46:1-10.
 111. Neicu T, Shirato H, Seppenwoolde Y, Jiang SB. Synchronized moving aperture radiation therapy (SMART): Average tumour trajectory for lung patients. *Phys Med Biol* 2003;48:587-98.
 112. Papiez L. The leaf sweep algorithm for an immobile and moving target as an optimal control problem in radiotherapy delivery. *Math Comput Model* 2003;37:735-45.
 113. Papieza L. DMLC leaf-pair optimal control of IMRT delivery for a moving rigid target. *Med Phys* 2004;31:2742-54.
 114. Papiez L, Rangaraj D. DMLC leaf-pair optimal control for mobile, deforming target. *Med Phys* 2005;32:275-85.
 115. Papiez L, Rangaraj D, Keall P. Real-time DMLC IMRT delivery for mobile and deforming targets. *Med Phys* 2005;32:3037-48.
 116. Papiez L, McMahon R, Timmerman R. 4D DMLC leaf sequencing to minimize organ at risk dose in moving anatomy. *Med Phys* 2007;34:4952-6.
 117. Webb S. The effect on IMRT conformality of elastic tissue movement and a practical suggestion for movement compensation via the modified dynamic multileaf collimator (dMLC) technique. *Phys Med Biol* 2005;50:1163-90.
 118. Webb S. Limitations of a simple technique for movement compensation via movement-modified fluence profiles. *Phys Med Biol* 2005;50:N155-61.
 119. Webb S. Does elastic tissue intrafraction motion with density changes forbid motion-compensated radiotherapy? *Phys Med Biol* 2006;51:1449-62.
 120. Webb S, Binnie DM. A strategy to minimize errors from differential intrafraction organ motion using a single configuration for a 'breathing' multileaf collimator. *Phys Med Biol* 2006;51:4517-31.
 121. Webb S. Quantification of the fluence error in the motion-compensated dynamic MLC (DMLC) technique for delivering intensity-modulated radiotherapy (IMRT). *Phys Med Biol* 2006;51:L17-21.
 122. Webb S. Intrafraction motion compensation by highly constrained iterative deconvolution of organ motion. *Phys Med Biol* 2007;52:N309-20.
 123. Webb S, Bortfeld T. A new way of adapting IMRT delivery fraction-by-fraction to cater for variable intrafraction motion. *Phys Med Biol* 2008;53:5177-91.
 124. Webb S. Adapting IMRT delivery fraction-by-fraction to cater for variable intrafraction motion. *Phys Med Biol* 2008;53:1-21.
 125. McClelland JR, Webb S, McQuaid D, Binnie DM, Hawkes DJ. Tracking 'differential organ motion' with a 'breathing' multileaf collimator: Magnitude of problem assessed using 4D CT data and a motion-compensation strategy. *Phys Med Biol* 2007;52:4805-26.
 126. Rangaraj D, Palaniswaamy G, Papiez L. DMLC IMRT delivery to targets moving in 2D in beam's eye view. *Med Phys* 2008;35:3765-78.
 127. McMahon R, Papiez L, Rangaraj D. Dynamic-MLC leaf control utilizing on-flight intensity calculations: A robust method for real-time IMRT delivery over moving rigid targets. *Med Phys* 2007;34:3211-23.
 128. McQuaid D, Partridge M, Symonds-Taylor JR, Evans PM, Webb S. Target-tracking deliveries on an Elekta linac: A feasibility study. *Phys Med Biol* 2009;54:3563-78.
 129. Sawant A, Venkat R, Srivastava V, Carlson D, Povzner S, Cattell H, *et al.* Management of three-dimensional intrafraction motion through real-time DMLC tracking. *Med Phys* 2008;35:2050-61.
 130. Tewatia D, Zhang T, Tome W, Paliwal B, Metha M. Clinical implementation of target tracking by breathing synchronized delivery. *Med Phys* 2006;33:4330-6.
 131. Tacke MB, Nill S, Krauss A, Oelfke U. Real-time tumor tracking: Automatic compensation of target motion using the Siemens 160 MLC. *Med Phys* 2010;37:753-61.
 132. Pollock S, Lee D, Keall P, Kim T. Audiovisual biofeedback improves motion prediction accuracy. *Med Phys* 2013;40:041705.
 133. Yi BY, Han-Oh S, Lerma F, Berman BL, Yu C. Real-time tumor tracking with preprogrammed dynamic multileaf-collimator motion and adaptive dose-rate regulation. *Med Phys* 2008;35:3955-62.
 134. Falk M, Munck af Rosenschöld P, Keall P, Cattell H, Cho BC, Poulsen P, *et al.* Real-time dynamic MLC tracking for inversely optimized arc radiotherapy. *Radiother Oncol* 2010;94:218-23.
 135. Sun B, Rangaraj D, Papiez L, Oddiraju S, Yang D, Li HH, *et al.* Target tracking using DMLC for volumetric modulated arc therapy: A simulation study. *Med Phys* 2010;37:6116-24.
 136. Davies GA, Poludniowski G, Webb S. MLC tracking for Elekta VMAT: A modelling study. *Phys Med Biol* 2011;56:7541-54.
 137. Davies GA, Clowes P, Bedford JL, Evans PM, Webb S, Poludniowski G, *et al.* An experimental evaluation of the agility MLC for motion-compensated VMAT delivery. *Phys Med Biol* 2013;58:4643-57.
 138. Zimmerman J, Korreman S, Persson G, Cattell H, Svatos M, Sawant A, *et al.* DMLC motion tracking of moving targets for intensity modulated arc therapy treatment: A feasibility study. *Acta Oncol* 2009;48:245-50.
 139. Wijesooriya K, Bartee C, Siebers JV, Vedam SS, Keall PJ. Determination of maximum leaf velocity and acceleration of a dynamic multileaf collimator: Implications for 4D radiotherapy. *Med Phys* 2005;32:932-41.
 140. Yoganathan SA, Maria Das KJ, Agarwal A, Kumar S. Performance evaluation of respiratory motion-synchronized dynamic IMRT delivery. *J Appl Clin Med Phys* 2013;14:4103.
 141. Yoganathan SA, Maria Das KJ, Agarwal A, Kumar S, Velmurugan J, Kumar S. Synchronization of Intra-fractional motion in dynamic IMRT delivery. *Int Fed Med Biol Eng* 2012;39:1923-5.
 142. Keall PJ, Cattell H, Pokhrel D, Dieterich S, Wong KH, Murphy MJ, *et al.* Geometric accuracy of a real-time target tracking system with dynamic multileaf collimator tracking system. *Int J Radiat Oncol Biol Phys* 2006;65:1579-84.
 143. Poulsen PR, Cho B, Sawant A, Ruan D, Keall PJ. Detailed analysis of latencies in image-based dynamic MLC tracking. *Med Phys* 2010;37:4998-5005.
 144. Hoogeman M, Prévost JB, Nuytens J, Pöll J, Levendag P, Heijmen B, *et al.* Clinical accuracy of the respiratory tumor tracking system of the cyberknife: Assessment by analysis of log files. *Int J Radiat Oncol Biol Phys* 2009;74:297-303.
 145. Fast MF, Nill S, Bedford JL, Oelfke U. Dynamic tumor tracking using the Elekta Agility MLC. *Med Phys* 2014;41:111719.
 146. Bedford JL, Fast MF, Nill S, McDonald FM, Ahmed M, Hansen VN, *et al.* Effect of MLC tracking latency on conformal volumetric modulated arc therapy (VMAT) plans in 4D stereotactic lung treatment. *Radiother Oncol* 2015;117:491-5.
 147. Booth JT, Caillet V, Hardcastle N, O'Brien R, Szymura K, Crasta C, *et al.* The first patient treatment of electromagnetic-guided real time adaptive radiotherapy using MLC tracking for lung SABR. *Radiother Oncol* 2016;121:19-25.